Analysis of 2-Dimensional Shallow Water Equations Using Multigrid Method and Coordinate Transformation

Jong-Seol Lee[1], Woncheol Cho[2]

[1] Project Manager, National Institute for Disaster Prevention, Ministry of Government Administration & Home Affairs, Seoul 121-719, Korea

[2] Professor, Dept. of Civil Engrg., Yonsei Univ., Seoul 120-749, Korea

(Manuscript received 26 October, 1998)

Abstract

Various numerical methods for the two dimensional shallow water equations have been applied to the problems of flood routing, tidal circulation, storm surges, and atmospheric circulation. These methods are often based on the Alternating Direction Implicit(ADI) method. However, the ADI method results in inaccuracies for large time steps when dealing with a complex geometry or bathymetry. Since this method reduces the performance considerably, a fully implicit method developed by Wilders et al. (1988) is used to improve the accuracy for a large time step.

Finite Difference Methods are defined on a rectangular grid. Two drawbacks of this type of grid are that grid refinement is not possible locally and that the physical boundary is sometimes poorly represented by the numerical model boundary. Because of the second deficiency several purely numerical boundary effects can be involved. A boundary fitted curvilinear coordinate transformation is used to reduce these difficulties. If the coordinate transformation is orthogonal then the transformed shallow water equations are similar to the original equations.

Therefore, an orthogonal coordinate transformation is used for defining coordinate system. A multigrid (MG) method is widely used to accelerate the convergence in the numerical methods. In this study, a technique using a MG method is proposed to reduce the computing time and to improve the accuracy for the orthogonal grid generation and the solutions of the shallow water equations.

1. Introduction

Various numerical models for the solution of the shallow water equation (SWEs) have been applied to the problems of stream flow and tidal circulation. Of these flow models, the finite difference model has been widely used because it is easier to deal with a time dependent term and computational time can be reduced.

Many of the existing finite difference models for the computation of the SWEs are based on the Alternating Direction Implicit (ADI) method. But the ADI method give rise to serious errors for large Courant numbers (larger than 5~10) and its numerical instabilities are intensified especially for the practical applications with complex geometric and bathymetric properties. To reduce the drawbacks of ADI method, Benque et al. (1982) and Wilders et al. (1988) proposed the fully implicit method which retains the accuracy for large time steps.

Because, in general, FDM is defined on rectangular grid, there are two types of major difficulties: Grid refinement in rapidly varied flow region is impossible and the physical boundaries are not represented by the numerical boundaries. Moreover, accurate approximation in the computational region is not expected because the errors are already introduced on boundaries. This deficiency is reduced by using boundary fitted curvilinear coordinate.

The curvilinear grid is generated by solving the elliptic partial differential equation iteratively. Also, fully implicit method needs on iteration procedure to satisfy the conservation of mass, and the efficiency of the algorithm is deteriorated by this procedure.

Therefore, in this study, more stable and efficient model will be established by complementing the deficiencies mentioned, and numerical tests will be performed to show the capabilities of the proposed model.

2. Governing Equations of 2-D Flow Model

The two dimensional SWEs can be derived from Reynolds equations. Assuming that vertical velocity and acceleration are much smaller than horizontal ones in shallow water flows, and integrating the 3-D system of Reynolds equations over water depth, SWEs on the Cartesian coordinate system can be easily derived.

Using the orthogonal coordinate transformation relationships, SWEs on the Cartesian coordinate system are transformed as,

$$\frac{\partial \zeta}{\partial t}+\frac{1}{\sqrt{g_*}}\frac{\partial}{\partial \xi}(Hu\sqrt{g_{22}})+\frac{1}{\sqrt{g_*}}\frac{\partial}{\partial \eta}(Hv\sqrt{g_{11}}) = 0, \tag{1}$$

$$\frac{\partial u}{\partial t}+\frac{u}{\sqrt{g_{11}}}\frac{\partial u}{\partial \xi}+\frac{v}{\sqrt{g_{22}}}\frac{\partial u}{\partial \eta}+\frac{uv}{\sqrt{g_*}}\frac{\partial \sqrt{g_{11}}}{\partial \eta}-\frac{v^2}{\sqrt{g_*}}\frac{\partial \sqrt{g_{22}}}{\partial \xi}+\frac{g}{\sqrt{g_{11}}}\frac{\partial \zeta}{\partial \xi}+f_B u=0, \tag{2}$$

$$\frac{\partial v}{\partial t}+\frac{u}{\sqrt{g_{11}}}\frac{\partial v}{\partial \xi}+\frac{v}{\sqrt{g_{22}}}\frac{\partial v}{\partial \eta}+\frac{uv}{\sqrt{g_*}}\frac{\partial \sqrt{g_{22}}}{\partial \xi}-\frac{u^2}{\sqrt{g_*}}\frac{\partial \sqrt{g_{11}}}{\partial \eta}+\frac{g}{\sqrt{g_{22}}}\frac{\partial \zeta}{\partial \eta}+f_B v=0, \tag{3}$$

where,

d is water depth below reference plane,

ζ is water level above reference plane,

H is total depth [= $\zeta + d$],

u and v are velocity components in x and y direction,

g_{11} is metric tensor component [= $(\partial x/\partial \xi)^2+(\partial y/\partial \xi)^2$],

g_{22} is metric tensor component [= $(\partial x/\partial \eta)^2+(\partial y/\partial \eta)^2$],

$\sqrt{g_*}$ is transformed Jacobian[= $\sqrt{g_{11}\cdot g_{22}}$],

f_B is bottom friction coefficient [= $gn^2\frac{\sqrt{u^2+v^2}}{(\zeta+d)^{4/3}}$], and

n is Manning's roughness coefficient.

The transformed shallow water equations (TSWEs) need to be solved in the orthogonal curvilinear grid system. These equations are similar to the SWEs on the Cartesian coordinate system since only two extra terms which take into account the curvature of transformation in momentum equations are included, and they are selected as governing equations in this study.

3. Orthogonal Curvilinear Grid Generation

To generate the orthogonal coordinates, Laplace equations were selected as,

$$\frac{\partial}{\partial \xi}\left(f\frac{\partial x}{\partial \xi}\right)+\frac{\partial}{\partial \eta}\left(\frac{1}{f}\frac{\partial x}{\partial \eta}\right)=0, \tag{4}$$

$$\frac{\partial}{\partial \xi}\left(f\frac{\partial y}{\partial \xi}\right)+\frac{\partial}{\partial \eta}\left(\frac{1}{f}\frac{\partial y}{\partial \eta}\right)=0, \tag{5}$$

where, the distortion function, f is expressed by the metric tensor function,

$$f^2(\xi,\eta)=\frac{g_{22}}{g_{11}}=\frac{x_\xi^2+y_\xi^2}{x_\eta^2+y_\eta^2}. \tag{6}$$

In the field solution approach by Laplacian, the distortion function involves the orthogonality and smoothness of generated grid. Thompson et al.(1985) presented several

rules for specifying f on the interior of the field given boundary values for f. However, if complete Dirichlet condition is desired, that is, if boundary coordinates on all sides are specified, it is more appropriate to consider equations (4) and (5) as a set of nonlinear, coupled PDEs. Here f is not predetermined but is calculated from its definition equation (6) in the course of the iteration solution. For this approach, the generating method proposed by Albert (1988) is used in this study. In this method, the values of the distortion function on the boundary are not required since the distortion function is defined not on grid point but on midpoint grid. These values are calculated in the course of the iterative solution according to equation (6) so that complete Dirichlet condition and nonlinearity of PDEs can be satisfied.

In this study, MG method is used to reduce the computing time and improve the convergency for solving the equations (4) and (5). Full approximation storage (FAS) scheme which can be applied to nonlinear problems without assuming the linearity is used because equations (4) and (5) are nonlinear Laplace equation of which the coefficients are functions of dependent variables as in equation (6). The ADI iterative method is used as the smoother in MG method.

4. Two-D Horizontal Flow Model

4.1 Staggered Grid System

In the computation of SWEs, dependent variables such as water level ζ, water depth d, and flow velocities u and v should be defined on the appropriate grid system. There are various types of staggered grid according to the location of each variable defined on the grid, and the staggered grid has been widely used because it has the advantages as follows: Various types of boundary condition can be easily implemented, and spurious oscillations whose wave periods are twice as the grid step size would not appear.

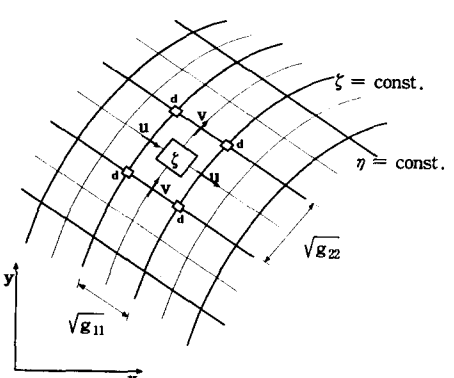

Figure 1. Basic Staggered Grid System

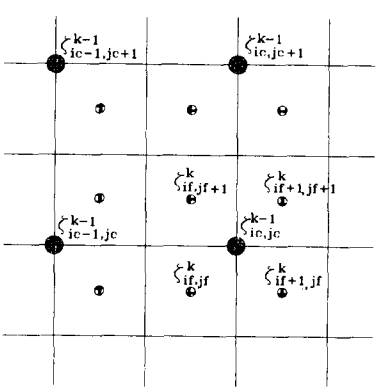

(a) Water Level Control Volume

Figure 1 shows the basic staggered grid system used in this study. The metric tensor coefficients have to be chosen on staggered grid, $\sqrt{g_{11}}$ and $\sqrt{g_{22}}$ were located at v and u velocity locations respectively. In multigrid system, locations of variables defined on the coarse grid are different to those defined on the fine grid. Figure 2 shows the relationship of the control volume between the fine and coarse grids.

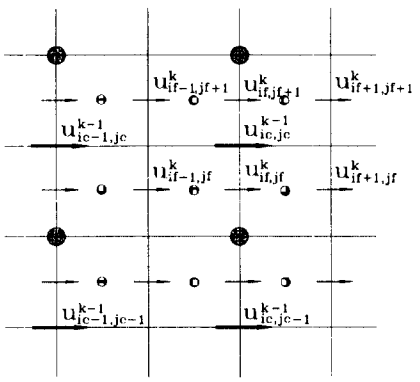

(b) Velocity u Control Volume

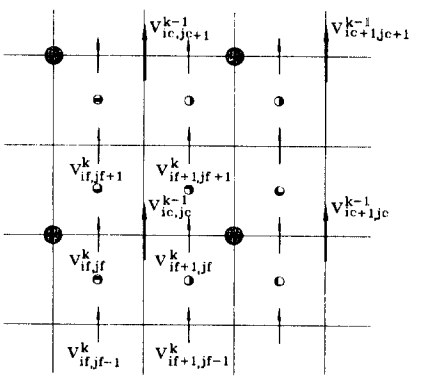

(c) Velocity v Control Volume

Figure 2. Relationship of the Control Volume between the Fine and Coarse Grids

4.2 Formulation of Finite Difference Equations

In a mathematical model, diffusion terms represented as effective shear stress terms were not included in the equation set, but their effects were considered by spatially weighted-averaging the variables defined on adjacent grid points. Also, Coriolis force term was not included because its effect is not important for this study. The difference equations are similar to those of Wilders (1988) except that the first order upwind scheme is used in differentiating the cross convective term. The computational procedures are as follows: In the first stage, conservative form of continuity equation (1) is solved explicitly, and uncoupled momentum equations (2) and (3) are then solved implicitly by an iterative method, respectively. In the second stage, explicit equations with respect to u and v are derived from equations (2) and (3), respectively, and they are coupled with the non-conservative form of continuity equation. To formulate the non-conservative form of Eq. (1), the following equation is used,

$$\frac{1}{\sqrt{g_*}}\frac{\partial}{\partial\xi}\left[(\zeta+d)u\sqrt{g_{22}}\right] = \frac{1}{\sqrt{g_*}}\left\{\frac{\partial}{\partial\xi}\left[du\sqrt{g_{22}}\right]+\zeta\frac{\partial}{\partial\xi}\left[u\sqrt{g_{22}}\right]+u\sqrt{g_{22}}\frac{\partial\zeta}{\partial\xi}\right\}, \tag{7}$$

and the second term of equation (1) is linearized resulting in a similar form to equation (7).

Therefore, the resulting system has only one unknown of water level. After the solution with respect to water level is obtained, velocities can be computed by substituting the result into the explicit form of the momentum equations (2) and (3). These solution processes are continued until the desired accuracy is achieved. The difference operators and the modified operators near boundaries are not described here. For details, refer to Stelling (1984) and Wilders et al. (1988).

4.3 Full Approximation Storage Scheme

It is well known that error components situated in low-frequency range are slowest to be damped in the iteration process although the higher frequencies are the first to be reduced and, after a few iteration, a large part of the high-frequency error components will generally be damped. The basic concept of MG method is to improve the convergency in such a way that one or more iteration apply to reduce the high-frequency error components represented on the fine grid until the error behavior is sufficiently smooth to be adequately represented on coarse grid and, after transfering the remaining errors from the fine grid to the coarse grid, low-frequency errors quickly smooth out on the coarse grid.

The MG method is classified as CS (Correction Storage) scheme and FAS (Full Approximation Storage) scheme according to the process working with full solution or only with the correction to the solution. In this study, FAS scheme is used for solving the generating equations referred in Section 3 and the resulting continuity equation of TSWEs and its procedures are as follows.

The conventional numerical method performs the computations on only one grid network (single-grid method). On the contrary, the computations by MG method are performed on a set of grids, i.e. G^k (k = 1, 2,....., M), where M is the finest grid level. Suppose that the grid size of k grid level is Δ_k, the exact discrete solution is U_k, the differential operator is L_k, and the source term is F_k, the differential equations on each grid G^k can be represented as:

$$L_k U_k = F_k. \tag{8}$$

The approximation of equation (8) is computed by a conventional relaxation method (i.e., smoother) such as GS, SOR, SSOR, Zebra, and Red-Black method etc. Unless the approximate solution u_k satisfies equation (8), the equation becames,

$$L_k u_k = f_k - R_k, \tag{9}$$

where R_k is the residuals of k grid level. Subtracting equation (9) from equation (8), the residual equation is obtained as,

$$L_k[u_k+\Delta u_k]-L_k[u_k]=F_k-f_k+R_k. \tag{10}$$

The fine grid residual equation (10) can be written on the coarse grid by restricting the residual and correction to form a corresponding equation as:

$$L_{k-1}[\Pi_k^{k-1}(u_k)+\Delta u_k]-L_{k-1}[\Pi_k^{k-1}(u_k)]=F_{k-1}-f_{k-1}+I_k^{k-1}(R_k), \tag{11}$$

where restriction operator Π_k^{k-1} for the approximate solution may be different from the restriction operator i_k^{k-1} for residual (Shyy et al., 1992). The equation (11) reduces to following equation (12) by putting the known quantities on the right-hand side,

$$L_{k-1}u_{k-1} = F_{k-1} + R_{k-1}, \tag{12}$$

where

$$u_{k-1} = \Pi_k^{k-1}(u_k)+\Delta u_k, \tag{13}$$

and

$$R_{k-1} = L_{k-1}[\Pi_k^{k-1}(u_k)] - f_{k-1} + I_k^{k-1}(R_k). \tag{14}$$

The decision to switch to finer grid or back to coarser grid depends on the internal check which is usually based on relative magnitude of residuals (Brandt et al., 1977). If the smoothing rate is low, which can be expressed as:

$$R^{[q]}/R^{[q-1]} > \tilde{\mu}, \tag{15}$$

then the current approximation to the solution is restricted to a coarser grid. In equation (15), $R^{[q]}$ denotes the average change of the approximation from the [q-1] iteration step to the [q] step and RA is a constant. The amount of work unit required, which is equivalent to the finest grid iterations, is almost the same for any RA in the range 0.2~0.8 and in this study RA is set to be 0.6 (Brandt et al., 1977 and Thompson et al., 1989). It is called FAS scheme, since the complete solution, not just the correction, is computed in calculating equation (10) on coarse grid.

The transfer process from finer grid to coarser grid is performed when

$$\varepsilon^{k-1} < \delta\varepsilon^k, \tag{16}$$

where,

$$\varepsilon^k = \sqrt{\frac{1}{N}\sum(u_k^{[q]}-u_k^{[q-1]})^2}. \tag{17}$$

The notation ϵ^k denotes root mean square error and N is the number of grid points, and superscript (q) is the iteration number.

The δ in equation (16) is the parameter which determines convergence rate for the solution on the coarser grid before the correction of the solution on finer grid solution. If it is too large, the elimination of low-frequency error components is ineffective on coarser grid, while it is too small, some of the coarser grid work will be wasted (Brandt et al., 1977 and Thompson et al., 1989). In this study, the value of B is set to be 0.3. Any value in the range 0.1~0.5 has little effect on the overall convergence rate. After solving equation (10), if equation (16) is true, the fine grid solution is updated by using,

$$u_k^{new} = u_k^{old} + I_{k-1}^k(u_{k-1} - I_k^{k-1}u_k^{old}), \tag{18}$$

where I_k^{k-1} denotes prolongation operator, and it is usually based on bilinear interpolation in two dimensions. Equation (18) represents interpolating the approximate correction on coarse grid and adding to the intermediate solution on the fine grid. Since the source term and the coefficient matrix on the coarse grid can be continuously updated to reflect progress made to the dependent variables, FAS scheme is very useful in solving the nonlinear problems.

4.4 Application of MG Method to SWEs

Momentum equations in the first stage and continuity equation in the second stage should be solved by an iteration method because these equations have an implicit difference equation form. While the solutions of momentum equations in first stage are achieved by only a few iteration, large computing time is required to calculate the resulting continuity equation in the second stage. Therefore MG method is applied to the iteration process in the second stage for solving TSWEs to improve the model efficiency. The SSOR method is used as the smoother of the MG method in the second stage as well as the iterative method in the first stage for solving TSWEs. The SSOR method alternates SOR sweeps in both directions. Hence, the SSOR method requires twice as much work as SOR, and it converges twice as fast.

Although the basic concepts of prolongation and restriction remain the same, the actual forms of the transfer operators are slightly different for each of the dependent variables as well as the corresponding residuals because the staggered grid system is employed for the velocities, water level, and water depth. Wesseling (1992) made the restrictions for the velocities and water level by averaging the nearby 6- and 4-point fine grid values, respectively, and the prolongations is achieved by applying bilinear interpolation from the coarse grid values (Figure 4). Ghia et al. (1988) and Shyy et al. (1992) conduct the restriction and prolongation through area weighting procedures, which is similar to the method presented by Wesseling (1992). In this study, the restriction operators presented by

Wesseling (1992) are used, and having the notation in Figure 4, the restrictions for water level and u-velocity are,

$$\zeta_{ic,jc} = I_k^{k-1}\zeta^f = \frac{1}{4}(\zeta_{if,jf}+\zeta_{if+1,jf}+\zeta_{if,jf+1}+\zeta_{if+1,jf+1}), \tag{19}$$

and

$$\begin{aligned} u_{ic,jc} &= I_k^{k-1}u^f \\ &= \frac{1}{4}(u_{if,jf}+u_{if,jf+1}) + \frac{1}{8}(u_{if+1,jf+1}+u_{if-1,jf+1}+u_{if+1,jf-1}+u_{if-1,jf-1}). \end{aligned} \tag{20}$$

The restriction for v-velocity is similar to equation (20). The prolongation operators for water level and velocity are expressed by

$$\begin{aligned} \zeta_{if,jf+1} &= I_{k-1}^{k}\zeta^c \\ &= \frac{1}{16}(9\zeta_{ic,jc}+3\zeta_{ic-1,jc}+3\zeta_{ic,jc+1}+\zeta_{ic-1,jc+1}), \end{aligned} \tag{21}$$

and

$$\begin{aligned} u_{if-1,jf} &= I_{k-1}^{k}u^c \\ &= \frac{1}{8}(3u_{ic,jc}+3u_{ic-1,jc}+u_{ic,jc-1}+u_{ic-1,jc-1}). \end{aligned} \tag{22}$$

The MG method is classified as a cycling algorithm and FMG (Full MultiGrid algorithm) according to the process beginning with the coarsest grid or with the finest grid. FMG is the solution process which starts with an approximate solution on coarsest grid. After the process of relaxation, restriction, and prolongation, the final solution on finest grid is obtained. On the other hand, cycling algorithm is the solution process which starts with an approximate solution on finest grid, and follows the process of relaxation, restriction, and prolongation to the coarsest grid and back again to obtain the solution on the finest grid.

The processes of relaxation, restriction, and prolongation according to the internal check of equations (15) and (16) are continued until the following equation (23) is satisfied on the finest grid.

$$\max\left[\sqrt{\sum_{i,j}(R_\zeta^M)_{i,j}^2\Delta\xi\Delta\eta}, \sqrt{\sum_{i,j}(R_\zeta^M)_{i,j}^2\Delta\xi\Delta\eta}, \sqrt{\sum_{i,j}(R_\zeta^M)_{i,j}^2\Delta\xi\Delta\eta}\right] < \tilde{\varepsilon} \tag{23}$$

where $\tilde{\varepsilon}$ with 5×10^{-4} represents a tolerance on the finest grid, and the same value is used in all experiments. For this study the cycling MG is found to be better than FMG because the computation of the resulting continuity equation starts from the approximations of the first stage. Hence, cycling MG is used, and it is applied only in the second stage.

5. Model Applications

5.1 Polar Basin

The flow model developed in this study is tested by comparing its results with analytical solutions by Lynch and Gray (1978). With polar and rectangular section, they present the analytical solutions for the linearized SWEs. They obtained from full SWEs by neglecting the convective terms, assuming the oscillations of the free surface are small compared to the total depth and using a linearized friction term. In this study, an experiment for a polar-shaped basin with constant bottom slope is performed as shown in Figure 3.

In the experiment, the depth of 3m is kept constant, and linearized bottom friction and wind stress are neglected. The basin has three sides that are closed. The tidal forcing function is specified at outer open boundary and is considered as cosine function with tidal period of 86,400 sec and tidal amplitude of 0.1 m. In Figure 3, the inner and outer radius

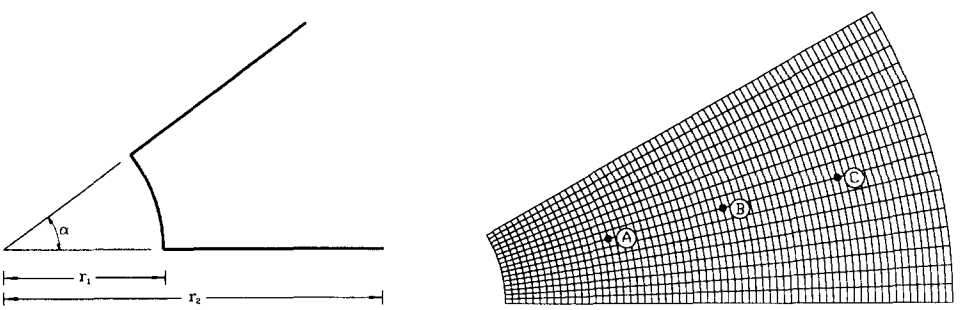

Figure 3. Computational grid of a polar basin

are 2.0 km and 8.4 km, respectively. The checkpoints A, B, and C at the distance of 3.6, 5.3, and 7.0 km from the origin of the coordinates are selected. The comparisons of the computed water level and velocity with analytical solutions are made during ten periods of the tidal wave at these points.

The time steps used in experiments were 300 sec (Cr=3), 900 sec (Cr=9), 3,600 sec (Cr=34), 4,800 sec (Cr=46), and 6,000 sec (Cr=57). In Figures 4 and 5, the computed results were compared with analytical solutions only at checkpoint A with the largest variation. While the results by the MG method were plotted for time steps of 300 sec, 3,600 sec, and 6,000 sec, the time steps greater than 4,800 sec in the SG method were not used because the computing times were very long even for the time step smaller than 4800 sec and their results were similar to that of MG method.

The time variation of computed and analytical solutions for water level at checkpoint A is plotted in Figure 4. Both results from MG and SG method were almost the same, and well agreed with analytical solutions. For Cr = 57, the maximum relative error was about 8% near the crest after one period, but its value reduced to about 1% after three periods.

Figure 5 shows the time variation of computed and analytical solutions for the velocity at checkpoint A. The overall time variation of the velocity agreed quite well with that of the analytical solution. The behavior of the velocity within 1~4 periods was unstable because a cold start is used as the initial condition. The Courant number has little influence on the results. Therefore, the proposed model can be used for practical problems.

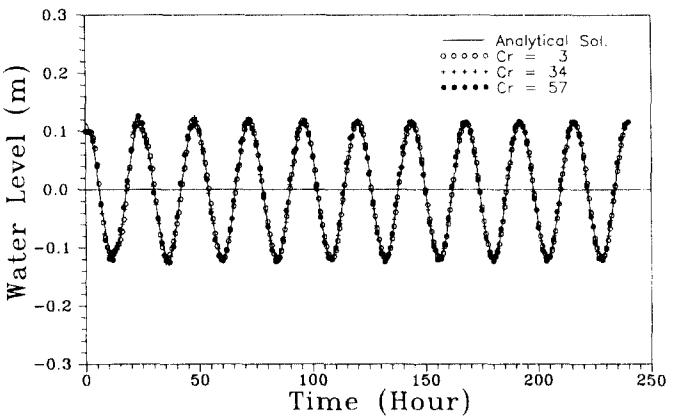

Figure 4. Comparison of Water Level between Analytical and Numerical Solutions

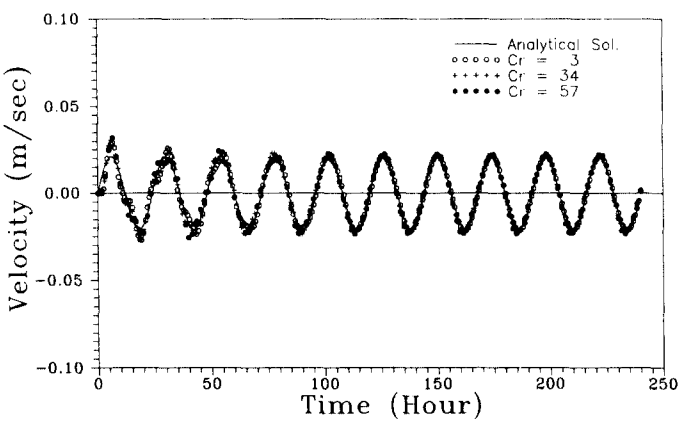

Figure 5. Comparison of velocities between analytical and numerical solutions

Table 1 shows the work unit and the total CPU time required in computations according to time steps. In the case of 300 sec, the MG procedure was less efficient than the SG procedure which does not need additional computations such as restriction and prolongation because a good approximation is achieved by only a few iteration when a small time step is used. However, the computational efficiency of the MG procedure increased as time steps increased, and the computational time of the MG method was 2.54 times faster than that of

the SG method when the time step is 3,600 sec. From the results of the experiment, it was concluded that 2-D flow model developed in this study is stable even for fairly large Courant number, and the efficiency of the model can be improved remarkably by applying the MG procedure.

Table 1. The Work Unit and Total Computing Time according to Time Steps

Time-step (second)	Courant No.	MG method (MG-SSOR)		SG method (SSOR)		Speed up rate
		Work unit	Total CPU time (CPUsec.)	Work unit	Total CPU time (CPUsec.)	
300	3	3~ 5	4,189.00	3~ 5	4,001.16	0.95
900	9	3~ 16	3,197.27	3~ 23	3,811.55	1.40
3,600	34	24~ 69	2,779.23	29~202	7,072.65	2.54
4,800	46	29~ 91	2,778.96	-	-	-
6,000	57	73~116	2,851.13	-	-	-

5.2 Dam Breaking

To show the capabilities of the proposed model, the test is performed on the region composed of channel part and floodplain part. This test is similar to that of Almeida and Franco (1993). As shown in Figure 6, the channel part is 5 m-wide and 50 m-long while the floodplain part is 40 m-wide and 31 m-long. It is assumed that sluice gate was located 34 m away from the end of channel upstream part, and the still water level difference between upstream and downstream part of the channel or floodplain is 2.5 m. The water depth of floodplain was 0.5 m. At the time, t = 0 sec, the initial flow velocity was 0 m/sec and the sluice gate is supposed to be opened instantaneously. It is known that majority of the numerical modeling is not adequate for this kind of situation, which has a discontinuous initial condition, because the effect of nonlinear portion of the equation increases. The computational grid size and time step were 1 m and 0.1 sec, respectively. It is assumed that the channel was frictionless and all the walls were set as closed boundary. Figure 6(a) shows the initial water level, and Figures from 6(b) to 6(f) depict the free surface change of the water with time. As shown in Figure 6(b), which show the water level at 0.5 sec after instantaneous opening of sluice gate, high velocity is generated because of the steep slope of water surface. Figure 6(c) depicts the water level after 1.5 sec. The channel flow is well developed and the surface is oscillating at upstream of the bore. The abrupt expansion leads to a diffraction of the wave that spreads circularly as shown in Figures 6(d) and 6(e). As shown in Figure 6(f), two shocks were created by the expansion waves reflected at the lateral wall boundaries of the floodplain. The results agreed well with that of Almeida and Franco (1993).

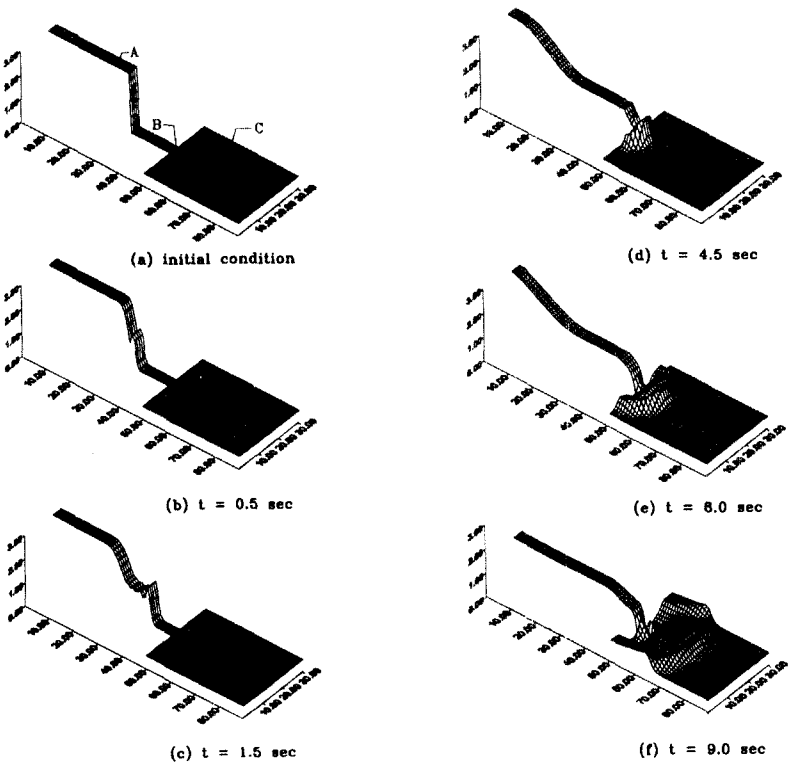

Figure 6. Time variation of free surface by dam breaking

6. Conclusions

In this study, the characteristics and applicabilities of the multigrid (MG) method, one of the accelerating numerical techniques, were examined, and the effective orthogonal grid generation model was established based on this method. Also, two dimensional flow model, which was based on the orthogonal coordinate systems and the fully implicit method, was established. In addition, the MG method was applied to improve the model efficiency.

The established model was tested using the problems for a polar basin and a dam breaking. The numerical solutions for the polar basin were compared with analytical ones. The results showed good accuracy and stability of the model even for the large Courant numbers. When the MG method was applied, the computing time was reduced to the maximum 2.5 times compared with the SG method. The proposed model was also applied to the analysis of a dam break flow with the strongly discontinuous initial condition, and the results were well agreed with other researchers'.

The verification of the model for real world problems should be performed, and it is expected that the proposed model results in reasonable approximations for real world problems.

References

Albert, M.R., Orthogonal curvilinear coordinate generation for internal flows, *in Numerical grid generation in computational fluid dynamics '88, Sengupta, S., et al. eds.*, Pineridge, Swansea, 425-433, 1988.

Almeida, R.J. and Franco, A.B., Modeling of dam-break flow, *in Computer Modeling of Free-Surface and Pressurized Flows, eds. Chaudhry, M.H. and Mays, L.W., NATO ASI Series*, 274, 343-373, 1993.

Benque, J.A., Cunge, J.F., Hauguel, A., and Holly, F.M., New method of tidal current computation, *J. of Waterway, Port, Coastal and Ocean Eng. Div., ASCE*, 108, WW3, 396-417, 1982.

Brandt, A., Multi-level adaptive solutions to boundary-value problems, *Math. of Comp.*, 31, 138, 333-390, 1977.

Ghia, U., Ramamurti, R., and Ghia, K.N., Solution of the Neumann pressure problem in general orthogonal coordinates using the multigrid techniqu, *AIAA J.*, 26, 5, 538-547, 1988.

Lynch, D.R., and Gray, W.G., Analytical solutions for computer flow model testing, *J. of Hydraulics Div., ASCE* 104, HY10, 1409-1428, 1978.

Shyy, W., Chen, M.H., and Sun, C.S., Pressure-based multigrid algorithm for flow at all speeds, *AIAA J.*, 30, 11, 2660-2669, 1992.

Stelling, G.S., On the construction of computational methods for shallow water flow problem, *Ph. D. Thesis*, Delft University, 1984.

Thopson, M.C. and Freziger, J.H., An adaptive miltigrid technique for the incompressible Navier-Stokes equation, *J. of Comp. Phys.*, 82, 94-121, 1987.

Thopmson, J.F., Wari, Z.U.A., and Mastin, C.W., Numerical grid generation, foundation and applications, North-Holland, New York, 1985.

Wesseling, P., An introduction to multigrid methods, John Wiley & Sons, 1992

Wilders, P., van Stijn, Th. L., Stelling, G.S., and Fokkema, G.A., A fully implicit method for accurate tidal computations, *Intern'l J. for Numer. Methods in Eng.*, 26, 2707-2721, 1988.